



New-Concept Gas Turbine Burner Simulation in Moderate Intense Low-Oxygen Combustion Regime

A. Di Nardo[†] and G. Calchetti

ENEA, Italian National Agency for New Technologies Energy and Sustainable Economic Development, Rome, via Anguillarese 301, 00123, Italy

[†]Corresponding Author Email: antonio.dinardo@enea.it

(Received November 22, 2016; accepted July 9, 2017)

ABSTRACT

In a trapped-vortex combustor (TVC) flame stabilization is achieved through intense internal exhaust gases recirculation, which is promoted by the adoption of cavities. Thanks to its peculiar features, a trapped-vortex burner produces low pressure drop and emissions and it is characterized by extended blow-out limits. The strong mixing of fresh reactants with flue gases due to internal recirculation represents the basis for the establishment of a distributed MILD, i.e. "Moderate Intense Low-Oxygen Dilution Combustion" regime, which is characterized by reduced temperature peaks, volumetric distributed reactions, low NO_x emissions and no thermo-acoustic instabilities. Aim of the work is to study the possibility to obtain a MILD regime in our available trapped-vortex device, taking the advantage of the combined effect of TVC strong internal exhaust gases recirculation and of oxy-combustion external exhaust recirculation, attaining the benefits of CO₂ capture at the same time. To this end a series of computational fluid dynamics simulations were conducted on our TVC device, in order to understand the influence on combustion of the main operating parameters, such as the equivalence ratio, the level of dilution, the injection temperature, the velocity, etc.. A preheating temperature and a range of oxygen concentrations that at the same time complies with a distributed reactions regime and an efficient combustion were identified for the premixed and non-premixed operating modes.

Keywords: Trapped-vortex burner; MILD combustion.

NOMENCLATURE

a	radiation absorption coefficient	Y_k^*	species mass fraction at the end of reaction
C	linear-anisotropic phase function coefficient		
D_k	molecular diffusion coefficient	$\alpha_k, \alpha_\epsilon$	inverse Prandtl numbers for k and ϵ
ER	equivalence ratio	Γ	G equation constant
G	incident radiation	ϵ	turbulent dissipation rate
G_k, G_b	generation of turb. kin. energy	μ_{eff}	sum of molecular and turbulent viscosity
J_j^k	turbulent diffusive flux	μ_t	turbulent viscosity
k	turbulent kinetic energy	μ	molecular viscosity
k_{eff}	effective thermal conductivity	ν	kinematic viscosity
K_v	recirculation factor	ζ^*	Kolmogorov length scale
p	pressure	ρ	density
q_r	radiative heat flux	σ	Stefan-Boltzmann constant
R_k	source term species equation	σ_s	scattering coefficient
R_ϵ	extra term ϵ equation	τ^*	reaction time scale
S	source term in energy equation	τ_{ij}	stress tensor
Sc_t	turbulent Schmidt number	$T, T_{max}, T_{in}, T_{si}$	temperature, temperature peak, inlet temperature, self-ignition temperature
t	time		
u_i	velocity component		
u_i'	fluctuating velocity component		
Y_M	compressibility effect in k equation		
Y_k	species mass fraction		

1. INTRODUCTION

In conventional burners the marked temperature gradient allows the triggering of radical chain reactions which are the basis of combustion. This condition is normally reached in the region of the flame front that separates reactants from products. The stability of this front, maintained thanks to a stable balance between flame speed and flow rate, with respect to fluctuations related to turbulence, is an essential requirement.

The term MILD (Moderate Intense Low-Oxygen Dilution Combustion) (Cavaliere and De Joannon 2004), refers to a combustion technique which uses high dilutions of the reactants mixture with inert gases, typically exhaust, in combination with high preheating temperatures. The strong dilution causes low oxygen concentration and the composition of the mixture to be outside the flammability limits, hence the necessity of preheating the incoming flow above the self-ignition temperature. In addition, the lowest possible temperature gradients limit the production of NO_x . Also soot formation is inhibited because of the lean conditions in the combustion chamber. The presence of a flame front is no longer necessary if the reactants are preheated above their self-ignition temperature, because the entire reaction volume is in conditions to react and to sustain the process. Then all the reactions take place in a wider volume, in absence of ignition and extinction phenomenon, due to the small temperature difference between burned and unburned gases, and the flame is no longer visible. For this reason MILD combustion it is also called flameless, (Wunning and Wunning 1997), or colorless, (Khalil *et al.* 2013), combustion by the different authors. The temperature homogeneity within the combustion chamber can also favor heat transfer control. Dilution with flue gases can be obtained directly into the combustion chamber by a proper design of the entire system and/or using oxygen enriched exhaust gases as oxidizer. The absence of a flame front removes one of the possible sources of thermo-acoustic instabilities.

The MILD technology has found many applications for furnaces on industrial scale but only laboratory scale examples exist for gas turbines, where actually MILD combustion has been not fully implemented and there are still open issues. There are in fact some complications in the gas turbines case. Since gas turbines burners work in strong excess of air, the flue gases still contain a high concentration of oxygen which makes it difficult to dilute the mixture to the desired levels. On the contrary, the strong heat transfer presents in furnaces, with the consequent reduction of temperatures, allows to work in almost stoichiometric conditions. Furthermore, the higher operating pressures and the higher temperatures in gas turbines burners, intensify the reaction rate and shorten the reaction time, favoring the presence of a flame front. In addition, the power density is much more intense with shorter residence times, that means less space and time to achieve the dilution required before the reaction begins. One of the first

examples of an experimental flameless burner for gas turbines was designed and tested by Levy and Sherbaum (2003). It was a pressurized circular sector of 60° , in which an air flow promotes the formation of a vortex which determines the recirculation of the hot combustion products. Although NO_x emissions were extremely low, high levels of carbon monoxide were found. At the DLR (Lucknerath *et al.* 2008) was experimented a burner operating in pressure and power density conditions typical of gas turbines (20 bar and 14.8 MW/m³bar). The combustor was provided with optical accesses and it was equipped with 12 high speed injectors of air and methane, circularly arranged in order to promote vortex formation and strong internal flue gases recirculation. It was shown how high speed injections produce an effective and intense mixing. For a preheating temperatures of about 700 K and an air-fuel equivalence ratio >2.1 , the flame was distributed over a large volume, the temperature was fairly uniform and low emissions were measured, up to the blowout limit. Researchers at the University of Maryland (Khalil *et al.* 2013) directed their studies toward the development of high power density burners, operating under colorless distributed combustion, aiming to increase efficiency, reduce the volume and equipment costs. They evaluated different configurations of premixed and non-premixed injections and flow patterns, able to increase mixing of fresh reactants and flue gases. Huang *et al.* (2014), evaluated the effect of the preheating temperature, for a parallelepiped MILD burner powered by four syngas lateral jets and four central air jets at high speed, arranged in a configuration which enhances mixing with combustion products. They identified the operating conditions in terms of equivalence ratio and velocity inlet which were able to produce a MILD combustion regime.

As emerges from the discussion above, the internal exhaust gases recirculation represents one of the possible strategies for a MILD regime. In fact it increases reactants temperature and diminishes the concentration of oxygen if a rapid and effective mixing takes place before the starting of reactions. The internal recirculation of exhaust gases is the key characteristic of a trapped-vortex burner (TVC). In conventional burner flame stabilization is achieved by means of swirl systems, which are able to produce hot gases entrainment toward the fresh mixture, supplying energy for flame sustainment. In the burners based on the trapped-vortex principle, the recirculation is guaranteed by vortices generated using cavities. If the system is properly designed, the vortex is stable inside the cavity or "trapped". The adoption of cavities for flame stabilization makes the entire device less sensitive to changes in the injections characteristics or in the operating conditions and suitable to operate at very lean stoichiometry. Vortices have been widely used in fluid-dynamic for different purposes. Many studies were conducted on can type burners, in which cavities were obtained by mounting two disks in series on a common spindle. Fuel and air were injected into the cavity to form the pilot flame

which ignited a main premixed mixture. Hsu *et al.* (1998) were first to report using this feature to stabilize reactions in gas turbine combustors for aero-propulsion application. From the can type version, an annular type version burning liquid fuel, was later designed to meet the requirements of aeronautical gas turbine: injections strategies and dual-vortex cavity were tested. The work of the scientific community towards the development of TVC burners is still fervent. Yadav and Kushari (2009) reported an experimental study on a low aspect ratio dump combustor, showing how the vortices formation and evolution allows to stabilize the flame without a swirler, through the enhanced mixing of fuel and air. Agarwal and Ravikrishna (2011) tested a compact two-dimensional TVC rig, reproducing an annular combustion chamber. A lean premixed flow was stabilized by a rectangular cavity having a variable size, in which fuel and air were injected to form the pilot flame. The combustion stability was improved by the adoption of guides capable of guiding part of the main flow within the cavity. A CFD analysis was conducted by Ghenai *et al.* (2013) on a first generation like TVC, fueled by pure hydrogen and syngas. The increase of hydrogen concentration produced higher temperatures and NO_x emissions and a shift of the reaction zone towards the second cavity, in comparison with methane feeding.

In practice, MILD combustion can be facilitated if the dilution level and the equivalence ratio (i.e. oxygen concentration) can be tuned independently as it is in oxy-combustion, where oxygen enriched combustion products are used as oxidizer (Hammond and Spargo 2014). However, it is clearly preferable to work in conditions very close to the stoichiometric value, to limit the cost of oxygen production. This is not possible when air is used as oxidizer, since the concentration of oxygen is fixed at 21% by volume. The adoption of this technique in trapped-vortex like burners makes possible to obtain low oxygen concentrations in the combustion chamber, representing thus a good starting point for the establishment of a MILD regime, with some further advantages. In fact oxy-combustion represents one of the possible solutions to the problem of global warming, linked to greenhouse gases emissions, especially CO₂, since fuel is burned in pure oxygen atmosphere rather than air, producing combustion products made only of carbon dioxide and water vapor, which can be easily separated by condensation and it is considered probably the most promising technique in terms of efficiency and implementation on industrial scale, also for existing plant retrofitting. It is nowadays crucial to develop technologies able to cut down CO₂ emissions from the energy production plants, considering that other industrial processes are massive emitters, such as iron, steel, cement production. Carbon capture and storage (CCS) is becoming part of the mix of strategies available to cope with the increasing atmospheric concentration of anthropogenic CO₂.

Aim of the work is to take the advantage of the combined effect of TVC strong internal exhaust

gases recirculation and oxy-fuel external exhaust recirculation, to obtain a very diluted combustion regime, with low CO emissions and O₂ wastefulness, associated with the advantages related to CCS. Since our existing experimental facility designed for air combustion has to be modified to work in CO₂ oxygen-enriched combustion conditions, it is not yet possible to conduct an experimental campaign. Therefore, as a preliminary study, preparatory for future experimental activities, the burner functioning has been analyzed by means of CFD simulations. A sensitivity analysis has been conducted with respect to injection velocity, CO₂ dilution, equivalence ratio and inlet temperature, in order to identify the proper operating conditions for a volumetric distributed combustion regime.

2. EXPERIMENTAL SETUP

The installed experimental device was designed to realize a MILD air-combustion regime by means of the intense internal exhaust recirculation produced by a single vortex filling the entire combustion chamber. The vortex is stable if the inlets are properly positioned and the inlets momentum is well tuned. In Fig. 1. is reported a scheme of the complete apparatus, which reproduces a linear sector of an annular type burner. The burner has two identical perforated plates for reactants supply. A secondary air flow (A) is introduced from one external row of holes. Three internal rows of holes supply the vortex core with methane fuel (C) and two internal rows of holes in between, feed the combustion chamber with primary air (B). The system can supply a total amount of secondary air, primary air and fuel in the range 0-300 Nm³/h, 0-100 Nm³/h e 0-15 Nm³/h, respectively. Air can be heated up by means of a 45 kW electrical heater. The burner is equipped with two lateral and one upper quartz optical accesses (F-H) for laser measurements, pressure transducers and probes placed at the burner exit for temperature and species analysis. Additional details are reported in the Fig. 1.

3. SIMULATION MODELS

The simulations were performed by the finite-volume ANSYS-FLUENT™ package on the ENEA CRESCO HPC cluster, using 128 cores. For pressure and velocity coupling a segregated pressure based approach was selected. In particular in the SIMPLE method mass conservation is obtained by a pressure correction equation, derived from the continuity and the momentum equations. A second-order upwind scheme was used for interpolation of convection terms at cells face.

The steady RANS simulations were conducted using the two equations RNG *k-ε* model (Yakhot and Orszag 1986) for turbulence, which is more suitable for the present work, since is more accurate for rotating and swirling flows.

In fact with respect to the standard *k-ε*, the RNG *k-ε* includes an extra term R_ϵ in the ϵ dissipation rate

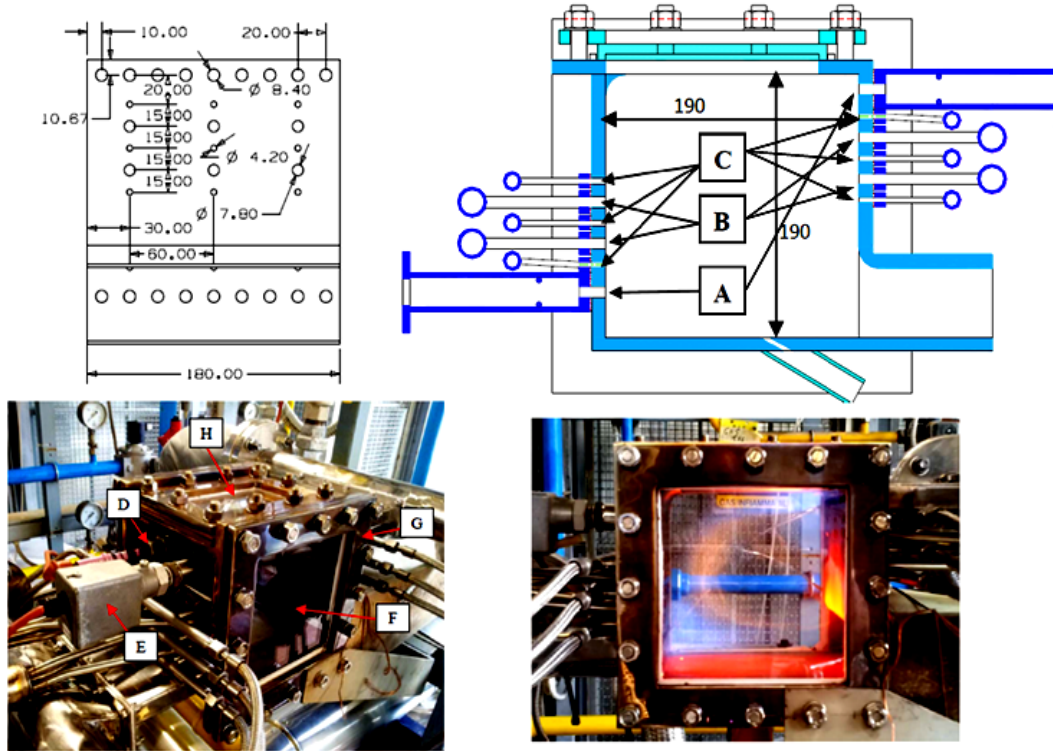


Fig. 1. Trapped-Vortex experimental facility. A secondary air, B primary air, C fuel, D spark ignition, E photocell, F-H quartz window, G steel flange.

equation, which improves the model for strained flows, the effect of swirl on turbulence, a formula for the turbulent Prandtl number and a formula for the eddy viscosity, which take into account low Reynolds number effects. In the MILD combustion regime the reaction rate is slow if compared to other regimes and the assumption of infinitely fast chemistry, where reactions time is faster than mixing, cannot be retained. For these reason the Eddy Dissipation Concept model (EDC), (Magnussen 1981), was applied for the calculation of the source terms in the species equations, in conjunction with the Smooke (Smooke *et al.* 1986) reduced reaction mechanism, made of 17 species and 46 reactions. The model supposes that reactions take place in the same small turbulent structures where the dissipation of turbulent energy occurs, called "fine structures", where the reactants are mixed at molecular level and are treated as perfectly stirred reactors.

Given the high concentration of CO₂, the gaseous medium is optically thick, which means that the gas is a high absorber and emitter in terms of radiation heat transfer. For this reason the P1 radiation model, (Siegel and Howell 1992), was applied for radiation, while the weighted sum of gray gas model (WSGGM), (Coppale and Vervisch 1983, Smith *et al.* 1982), was used for the calculation of the absorption coefficient a . The P1 model involves the solution of a single diffuse equation and then is less computational demanding than other models. It is based on the idea that the solution of the radiation heat transfer equation can be simplified by

expressing the radiation intensity as a series of products of angular and spatial functions.

In the following is reported a brief summary of the equations set.

Continuity

$$\frac{\partial \rho}{\partial t} + \frac{\partial}{\partial x_i}(\rho u_i) = 0 \quad (1)$$

Momentum

$$\begin{aligned} \frac{\partial \rho u_i}{\partial t} + \frac{\partial}{\partial x_j}(\rho u_i u_j) = -\frac{\partial p}{\partial x_i} + \\ + \frac{\partial}{\partial x_j} \left[\mu \left(\frac{\partial u_i}{\partial x_j} + \frac{\partial u_j}{\partial x_i} - \frac{2}{3} \delta_{ij} \frac{\partial u_l}{\partial x_l} \right) \right] + \frac{\partial}{\partial x_j} (-\rho \overline{u'_i u'_j}) \end{aligned} \quad (2)$$

where p is the static pressure, u is the mean velocity, u' is the fluctuating velocity, μ is the molecular viscosity and ρ is the density.

Turbulence

The Reynolds stresses in Eq. (2) using the Boussinesq formulas are:

$$-\rho \overline{u'_i u'_j} = \mu_t \left(\frac{\partial u_i}{\partial x_j} + \frac{\partial u_j}{\partial x_i} \right) - \frac{2}{3} \left(\rho k + \mu_t \frac{\partial u_k}{\partial x_k} \right) \delta_{ij} \quad (3)$$

In the equation above k is the turbulent kinetic energy and μ_t is the turbulent viscosity. The

equations for k and ε of the RNG model are then:

$$\frac{\partial}{\partial t}(\rho k) + \frac{\partial}{\partial x_i}(\rho k u_i) = \frac{\partial}{\partial x_j} \left(\alpha_k \mu_{eff} \frac{\partial k}{\partial x_j} \right) + G_k + G_b - \rho \varepsilon - Y_M \quad (4)$$

$$\frac{\partial}{\partial t}(\rho \varepsilon) + \frac{\partial}{\partial x_i}(\rho \varepsilon u_i) = \frac{\partial}{\partial x_j} \left(\alpha_\varepsilon \mu_{eff} \frac{\partial \varepsilon}{\partial x_j} \right) + C_{1\varepsilon} \frac{\varepsilon}{k} (G_k + C_{3\varepsilon} G_b) - C_{2\varepsilon} \rho \frac{\varepsilon^2}{k} - R_\varepsilon \quad (5)$$

here G_k and G_b are the generation of turbulent kinetic energy due to the mean velocity gradients and buoyancy, Y_M is related to compressibility effects, μ_{eff} is the sum of molecular and turbulent viscosity, $C_{1\varepsilon}=1.42$ $C_{2\varepsilon}=1.68$, $C_{3\varepsilon}$ is calculated and expresses how ε is influenced by buoyancy, α_k and α_ε are the inverse Prandtl numbers for k and ε . For further details on the calculation of these terms and the turbulent viscosity see [Yakhot and Orszag \(1986\)](#).

Species

$$\frac{\partial}{\partial t}(\rho Y_k) + \frac{\partial}{\partial x_j}(\rho u_j Y_k) = \frac{\partial J_j^k}{\partial x_j} + R_k \quad (6)$$

where Y_k is the species mass fraction, J_j^k is the turbulent diffusive flux:

$$J_j^k = - \left(\rho D_k + \frac{\mu_t}{Sc_t} \right) \frac{\partial Y_k}{\partial x_j} \quad (7)$$

here Sc_t is the turbulent Schmidt number, D_k the molecular diffusion coefficient, R_k is the source term due to reactions.

Energy

$$\frac{\partial}{\partial t}(\rho E) + \frac{\partial}{\partial x_i} [u_i (\rho E + p)] = \frac{\partial}{\partial x_j} \left(k_{eff} \frac{\partial T}{\partial x_j} + u_i (\tau_{ij})_{eff} \right) + S \quad (8)$$

where T is the temperature, S is a source term accounting for reactions and radiation, τ_{ij} is the stress tensor and k_{eff} the effective thermal conductivity.

Reaction rate

The source term R_k in the species Eq. (6) according to the EDC model is determined as:

$$R_k = \frac{\rho (\xi^*)^2}{\tau^* \left[1 - (\xi^*)^3 \right]} (Y_k^* - Y_i) \quad (9)$$

where Y_k^* is the species mass fraction after reaction

$$\xi^* = C_\xi \left(\frac{\nu \varepsilon}{k^2} \right)^{1/4} \quad (10)$$

is the fine structures Kolmogorov length scale, $C_\xi=2.1377$ and the reactions volume is ξ^{*3} . Reactions time scale is calculated as:

$$\tau^* = C_\tau \left(\frac{\nu}{\varepsilon} \right)^{1/2} \quad (11)$$

where $C_\tau=0.4082$.

Radiation heat transfer

The radiative heat flux source term ∇q_r in the Eq. (8) is calculated as:

$$-\nabla q_r = aG - 4a\sigma T^4 \quad (12)$$

where σ is the Stefan-Boltzmann constant. The incident radiation G transport equation is calculated from:

$$\nabla(\Gamma \cdot \nabla G) - aG + 4a\sigma T^4 = 0 \quad (13)$$

where Γ is:

$$\Gamma = \frac{1}{(3(a + \sigma_s) - C\sigma_s)} \quad (14)$$

σ_s is the scattering coefficient and C is a coefficient related to anisotropic scattering.

To limit the computational cost just a periodic module of the entire device has been simulated, using a tetrahedral mesh consisting in about 500 kcells, which was refined until no changes in the results were observed.

The set of the above described numerical models was validated on an experimental burner operating in MILD combustion conditions. The burner is a jet-in-hot co-flow (JHC), with a central fuel nozzle, a co-flow oxidant and a lateral air flow. The oxidant is a mixture of air and combustion products, with variable oxygen concentrations. The system was experimentally studied by [Dally et al. \(2002\)](#). The comparison of the radial profiles of some significant variables for the experiments named HM1 and HM3, has been reported in Fig. 2. In the paper can be found further details about the experimental conditions. The profiles were plotted at different distances (z) from the fuel nozzle. The agreement between the experimental data and the numerical simulations is quite good.

The aim of the CFD simulations was to find the burner working conditions that are able to produce a wide and distributed reaction zone and low CO emissions, with minimum O_2 consumption, i.e. equivalence ratio close to one. In this perspective the CFD results were analyzed in terms of few global parameters. The CO emission index, EICO, was used to compare pollutant emissions among the different cases.

The effectiveness of the internal mixing between fresh reactants and flue gases was assessed by calculating the recirculation factor K_v , defined as the ratio of the mass flow rate of internal recirculated burned gases and the mass flow rate of incoming fresh mixture. Since in MILD combustion temperature peaks are expected to be very small, the difference between maximum flame temperature and inlet temperature was evaluated. In addition, the reactive volume marked by the heat release was also examined. Two possible combustion modes,

premixed and non-premixed were tested. The complete set of the performed simulations is reported in Table 1 and 2.

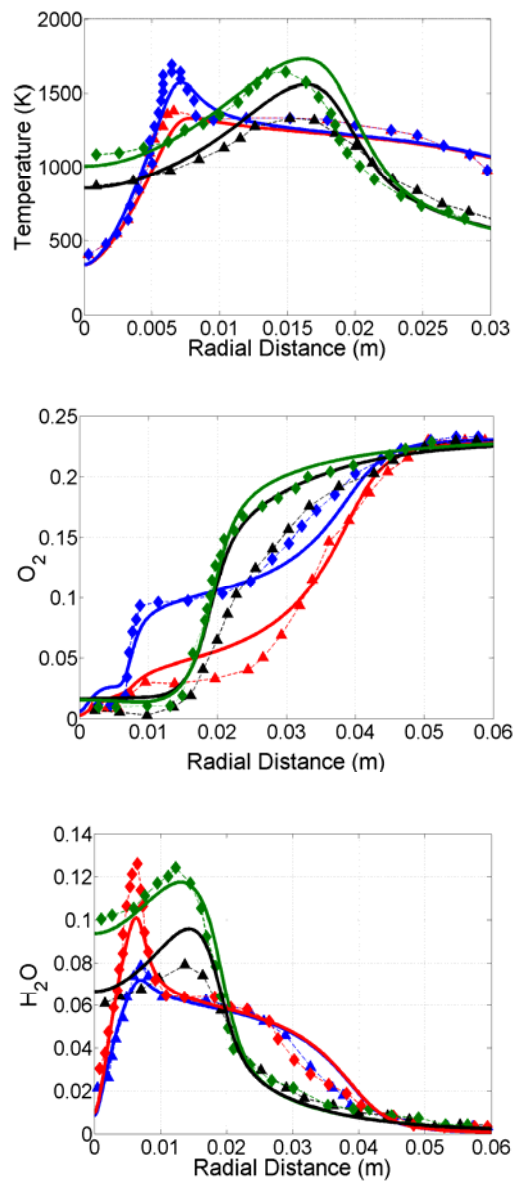


Fig. 2. Experimental (Dally *et al.* 2002) and numerical radial profiles comparison for models validation. HM1: \blacktriangle $z=30$ mm \blacktriangle $z=120$ mm. HM3: \blacklozenge $z=30$ mm \blacklozenge $z=120$ mm.

4. PREMIXED MODE RESULTS

In the premixed mode only the secondary air upper row of holes was used for the $CH_4/O_2/CO_2$ mixture injection, placed few millimeters distant from the original position (location A on the right in Fig. 1), with all the other injections closed. A sensitivity analysis was conducted with respect to injection velocity (40-100 m/s), oxygen concentration in the oxidizer (22-37%), equivalence ratio ($ER = (mCH_4/mO_2)/(mCH_4/mO_2)_{stoic} = 0.9, 0.95$) and injection temperature (470 and 870 K).

Table 1 Premixed combustion mode CFD cases

Case	ER	%O ₂	T _{in} (K)	v _{in} (m/s)
1	0.90	32	870	49
2	0.90	27	870	62
3	0.90	22	870	72.5
4	0.95	32	870	59.5
5	0.95	27	870	69.5
6	0.95	22	870	84.5
7	0.95	37	470	49.5
8	0.95	32	470	56
9	0.95	27	470	65.5
10	0.95	27	870	40
11	0.95	27	870	70
12	0.95	27	870	100

Table 2 Non-premixed combustion mode CFD cases

Case	ER	%O ₂	T _{in} (K)
1	0.87	23	870
2	0.87	19.5	870
3	0.87	17	870
4	0.82	23	870
5	0.82	19.5	870
6	0.82	17	870
7	0.87	23	470
8	0.87	19.5	470
9	0.87	17	470

For the case with the lower inlet temperature of 470 K, the injections diameter was reduced to maintain constant inlet velocities. The operating pressure was set at 4 bar and the fuel input power was 150 kW. Walls temperature was fixed at 1000 K in order to reproduce the cooling effect in a real apparatus. An example of temperature map is reported in Fig. 3.

From Fig. 4. it is clear that an increase of the O₂ level causes higher temperature peaks and a sharp reduction of CO in the exhaust gases, especially for low oxygen levels (22-27%) and for the higher equivalence ratio 0.95. One reason of the high emission index for the more diluted cases is the insufficient temperature levels for complete combustion. A second reason is the higher inlet velocity and then the lower residence time, that characterizes those cases. A O₂ increase causes a temperature rise, which better support combustion and causes the equilibrium reaction $CO+0.5O_2 \leftrightarrow CO_2$ to move right. A further increase over 32% would produce even higher temperatures, consequent higher CO₂ dissociation and the CO emissions growth. The greater amount of oxygen which characterizes the $ER=0.9$ cases, causes general lower emissions than the $ER=0.95$ cases.

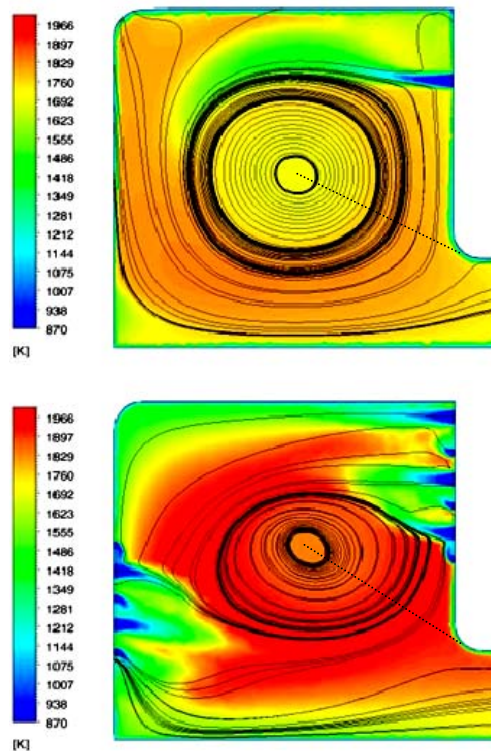


Fig. 3. Temperature (K) map and path lines. Top: Premixed mode $ER=0.95$, T_{in} 870 K, 27% O_2 . Bottom: Non-premixed mode $ER=0.87$, T_{in} 870 K, 23% O_2 .

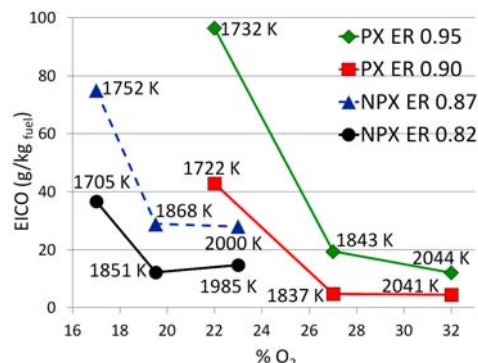


Fig. 4. CO emission index and maximum temperature as function of % O_2 in the oxidizer. Premixed mode: PX. Non-premixed mode: NPX. T_{in} 870 K.

The recirculation factor K_v , was calculated by evaluating the mass flow of the recirculating burned gases through the plane in Fig. 3 (dotted line), and reported in Fig. 5, as a function of the inlet velocity, at a fixed mass flow rate. K_v tends to grow rapidly in the low velocities range (40-70 m/s) and slowly at high velocities (70-100 m/s), while temperature peaks decrease almost linearly, due to the more intense mixing and dilution of the fresh mixture with the combustion products. This means that a further increase in the inlet velocity would produce only little changes in the recirculation factor. The burner is therefore able to promote a strong recirculation effect, as K_v reaches values even higher than 3.

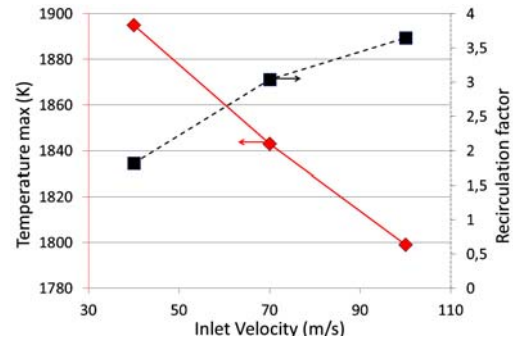


Fig. 5. Maximum temperature and recirculation factor K_v from CFD simulations as function of inlet velocity. T_{in} 870 K, ER 0.95, O_2 27%. Premixed mode.

As discussed in Cavaliere and De Joannon (2004), MILD combustion takes place if the maximum temperature increment ($T_{max}-T_{in}$) is smaller than the self-ignition temperature.

Figure 6 shows the temperature increment for some of the examined cases, compared with the self-ignition temperature (T_{si}), which is 1100 K, calculated by means of OpenSMOKE package, (Cuoci *et al.* 2011), for a homogenous closed reactor in a wide range of oxygen concentrations and for a maximum residence time of 40 ms. For an inlet temperature of 870 K and oxygen concentrations under 30%, the temperature increment is in fact inferior to the self-ignition temperature. Then in these conditions the criterion for MILD combustion regime is verified to be valid. The MILD combustion criterion is never valid for the injection temperature of 470 K. In fact, at lower inlet temperatures higher oxygen concentrations are required for flame sustainment and complete combustion, which inevitably causes higher temperature peaks and wider temperature increments.

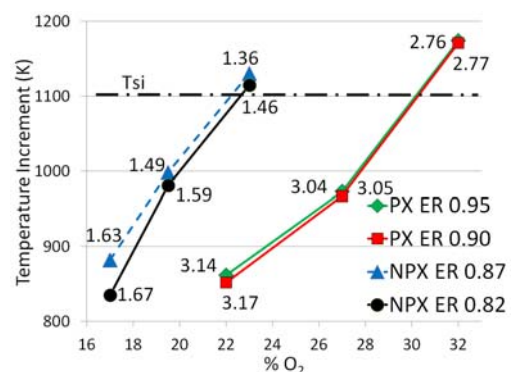


Fig. 6. Temperature increment and recirculation factor as function of % O_2 in the oxidizer. Premixed mode: PX. Non-premixed mode: NPX. T_{in} 870 K.

It is also interesting to evaluate the reactive volume (Figs. 7, 8 and 10), marked by the heat release, in fact the less intense is the heat release, the wider is the reaction zone. For the $T_{in}=870$ K cases, it results

that for O₂ concentration in the oxidizer up to 27%, the reacting volume and the heat release maximum are even four times wider with respect to the less diluted cases (O₂>27%). As reported in Fig. 8 and 9, the reaction zone width decreases rapidly for the less diluted cases (27-32% O₂) as oxygen is diminished and more slowly for the more diluted ones (22-27% O₂), while the heat release maximum behaves in opposite manner. In conclusion, in the cases with more intense preheating, the increase of oxygen up to 27% causes a beneficial reduction of CO emissions with a still low temperature increment and a wide volume of reaction.

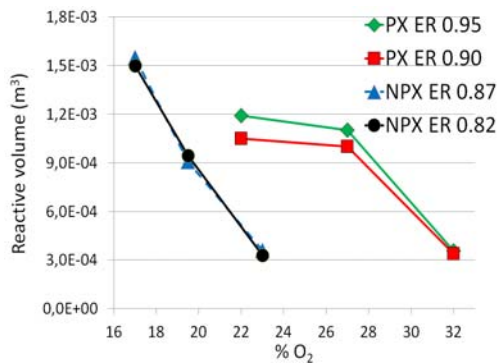


Fig. 7. Reactive volume as function of % O₂ in the oxidizer. Premixed mode: PX. Non-premixed mode: NPX. *T_{in}* 870 K.

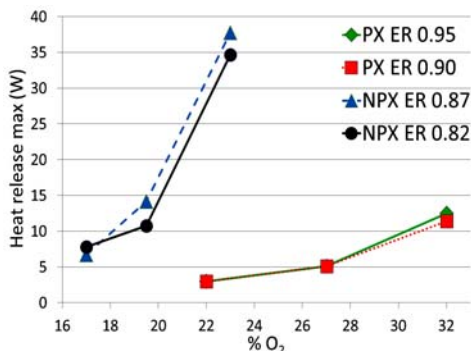


Fig. 8. Maximum heat release from CFD simulations as function of % O₂ in the oxidizer. *T_{in}* 870 K.

5. NON-PREMIXED MODE RESULTS

In the non-premixed mode the original burner configuration was studied. All the air injections were used for the CO₂/O₂ feeding, except for the lower secondary air inlet (location A on the left in Fig. 1). In this case the oxygen concentration was varied between 17% and 23%. As in the previous case, the operating pressure was set at 4 bar, the inlet temperatures were 470 K and 870 K and the fuel input power was fixed at 250 kW. Walls temperature was fixed at 1000 K. The equivalence ratio was set at 0.87 and 0.82, slightly inferior with respect to the premixed cases, to guarantee a

greater oxygen excess for a sufficient mixing and complete combustion since reactants are non-premixed. A sensitivity analysis to velocity was not performed since there are lots of injections in this case.

The temperature map (Fig. 3) shows general higher temperature levels than the premixed mode, as expected. From the Figs. 4, 6, 7 and 10 it is possible to gather similar considerations with respect to the premixed mode simulations. Also in the present case CO emissions are reduced as the oxygen concentration is increased, remaining almost constant for O₂ concentration over 19%, compared with the 27% of the premixed cases (Fig. 4). The lower equivalence ratio produces a CO emissions reduction, but clearly more oxygen consumption. The maximum temperature increment is inferior to the self-ignition temperature for O₂<22% and *T_{in}*=870 K, compared to the 30% for the premixed combustion (Fig. 6). As in the premixed case, for an inlet temperature of 470 K, the temperature increment is always superior to the self-ignition temperature.

The heat release peak (Figs. 7, 8 and 10) drops of about 5-6 times, as the oxygen concentration is diminished, while the reaction zone widens of about five times. Then, as expected, there is a greater sensitivity to oxygen levels with respect to the premixed mode. The recirculation factor doesn't exceed 1.67 but it is enough for a proper and effective dilution. In the end, at the higher preheating temperature of 870 K and for oxygen concentration in the oxidizer less than 22%, it seems that a MILD combustion regime is established.

6. CONCLUSIONS

A series of CFD simulations were executed to study MILD combustion in a trapped-vortex burner for gas turbines, operated in oxy-combustion. It was possible to identify the operating conditions for a MILD-like combustion regime, characterized by a considerable extension of the reaction zone and a substantial reduction of the heat release peaks. For a preheating temperature of 870 K the optimal oxygen concentration window that simultaneously assures a distributed combustion regime and low CO emissions, is centered around 27% and 19%, for the premixed and non-premixed operating modes, respectively. The lower equivalent ratio required by the non-premixed mode, needed to limit the CO emissions, implies an higher oxygen consumption with respect to the premixed case. In conclusion, the numerical analysis performed on the TVC burner gave encouraging results. In fact, the strong stabilization effect which characterizes the system allows to sustain the reaction at low flame temperatures and low oxygen concentrations, permitting the establishment of a volumetric distributed combustion regime with contemporary low emissions of unburned gases and minimum O₂ consumption.

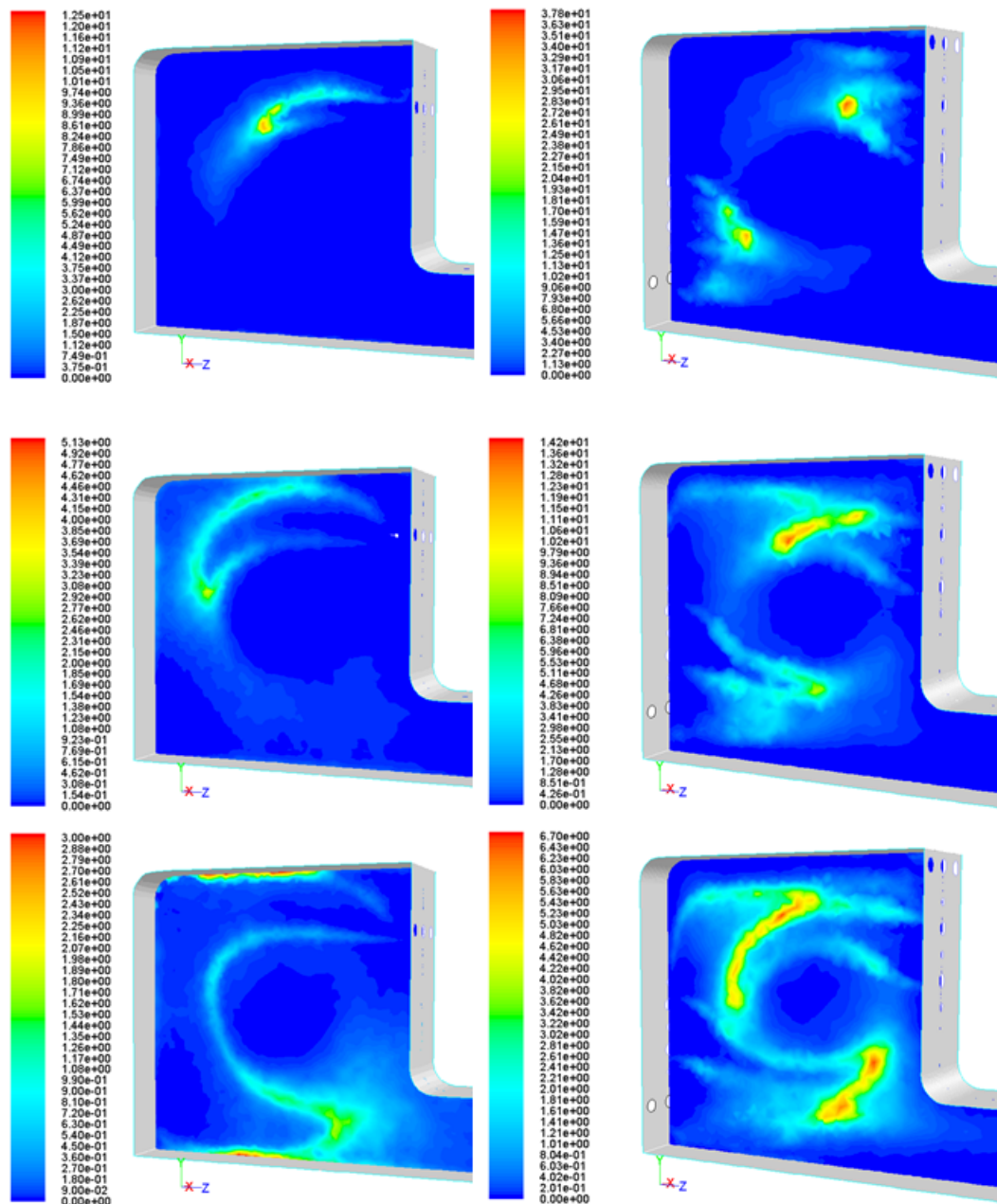


Fig. 9. Heat release map (W). Left: Premixed mode, $ER=0.95$, T_{in} 870 K, top 32% O_2 , middle 27% O_2 , bottom 22% O_2 . Right: Non-premixed mode, $ER=0.87$, T_{in} 870 K, top 23% O_2 , middle 19.5% O_2 , bottom 17% O_2 .

ACKNOWLEDGEMENTS

The computing resources and the related technical support used for this work have been provided by CRESO/ENEAGRID High Performance Computing infrastructure and its staff (Ponti *et al.* 2014). CRESO/ENEAGRID High Performance Computing infrastructure is funded by ENEA, the Italian National Agency for New Technologies, Energy and Sustainable Economic Development and by Italian and European research programs, see <http://www.cresco.enea.it/english> for information.

REFERENCES

- Agarwal, K. K. and R. V. Ravikrishna (2011). Experimental and numerical studies in a compact trapped vortex combustor: stability assessment and augmentation. *Combust. Sci. and Tech.* 183, 1308–1327.
- Cavaliere, A. and M. De Joannon (2004). MILD combustion”. *Progress in Energy and Combustion Science.* 30, 329-366.

- Coppalle, A. and P. Vervisch (1983). The total emissivities of high-temperature flames. *Combust. Flame* 49, 101-108.
- Cuoci, A., A. Frassoldati, T. Faravelli, E. Ranzi (2011). OpenSMOKE: Numerical modeling of reacting systems with detailed kinetic mechanisms. *XXXIV Meeting of the Italian Section of the Combustion Institute*.
- Dally, B. B., A. N. Karpetis, and R. S. Barlow (2002). Structure of turbulent non-premixed jet flames in a diluted hot coflow, *Proceedings of the Combustion Institut.* 29, 1147–1154.
- Ghenai, C., K. Zbeeb and I. Janajreh (2013). Combustion of alternative fuels in vortex trapped combustor. *Energy Conversion and Management* 65, 819–828.
- Hammond, G. P. and J. Spargo (2014), The prospects for coal-fired power plants with carbon capture and storage: A UK perspective. *Energy Conversion and Management* 86, 476–489.
- Hsu, K. Y., L. P. Goss and W. M. Roquemore (1998). Characteristics of a trapped vortex combustor. *Journal of Propulsion and Power*, 14, 57-65.
- Huang, M., Z. Zhang, W. Shao, Y. Xiong, Y. Liu, F. Lei, Y. Xiao (2014). Effect of air preheat temperature on the MILD combustion of syngas. *Energy Conversion and Management* 86, 356-364.
- Khalil, A. E. E., V. K. Arghode, A. K. Gupta, (2013). Novel mixing for ultra-high thermal intensity distributed combustion. *Applied Energy* 105, 327–334.
- Levy, Y. and V. Sherbaum (2003). Parametric study of the FLOXCOM combustor. *TAE Report No. 920, Technion*.
- Luckerath, R., W. Meier and M. Aigner (2008). FLOX® combustion at high pressure with different fuel compositions. *Journal of Engineering for Gas Turbines and Power* 130.
- Magnussen, B. F. (1981). On the structure of turbulence and a generalized eddy dissipation concept for chemical reaction in turbulent flow. *Nineteenth AIAA Meeting, St. Louis*.
- Ponti, G. *et al.* (2014). The role of medium size facilities in the HPC ecosystem: the case of the new CRESCO4 cluster integrated in the ENEAGRID infrastructure. *Proceedings of the 2014 International Conference on High Performance Computing and Simulation, HPCS 2014*, art. no. 6903807, 1030-1033.
- Siegel, R. and J. R. Howell (1992). Thermal Radiation Heat Transfer. *Hemisphere Publishing Corporation, Washington DC*.
- Smith, T. F., Z. F. Shen and J. N. Friedman (1982). Evaluation of coefficients for the weighted sum of gray gases model. *J. Heat Transfer* 104, 602-608.
- Smooke, M. D., I. K Puri and K. Seshadri (1986). A comparison between numerical calculations and experimental measurements of the structure of a counterflow diffusion flame burning diluted methane in diluted air. *Proceedings of the Combustion Institute* 21, 1783-1792.
- Wunning, J. A. and J. G. Wunning (1997). Flameless oxidation to reduce thermal NO formation. *Prog. Energy Combust Sci.*, 23, 81–94.
- Yadav, N. P. and A. Kushari (2009). Vortex combustion in a low aspect ratio dump combustor with tapered exit. *Energy Conversion and Management* 50, 2983–2991.
- Yakhot, V. and S. A. Orszag, (1986). Renormalization group analysis of turbulence: I. Basic theory. *Journal of Scientific Computing* 1(1), 1-51.